High-Power Targetry R&D for Next-Generation Accelerator Target Facilities

Abe Burleigh

NuFact 2024 - The 25th International Workshop on Neutrinos from Accelerators
16 September 2024
FERMILAB-SLIDES-24-0251-AD

High-power targetry (HPT) challenges

Next gen. multi-MW particle production accelerators expect ≈ 10X proton fluence & power density increase

- Target survivability concerns have led several facilities to limit beam power
  - NuMI-MINOS, FNAL (2010-11): faulty welds
    - Reduced beam power (-10% to -40%)
  - MLF, J-PARC (2015-16)
    - Early replacement of target/limited beam power
  - SNS, ORNL (2013-14)
    - Reduced beam power (-15%) frequently
- Radiation damage and thermal shock are the primary material challenges
- HPT critical for maximizing particle production efficiency

Neutrino HPT R&D Materials Exploratory Map

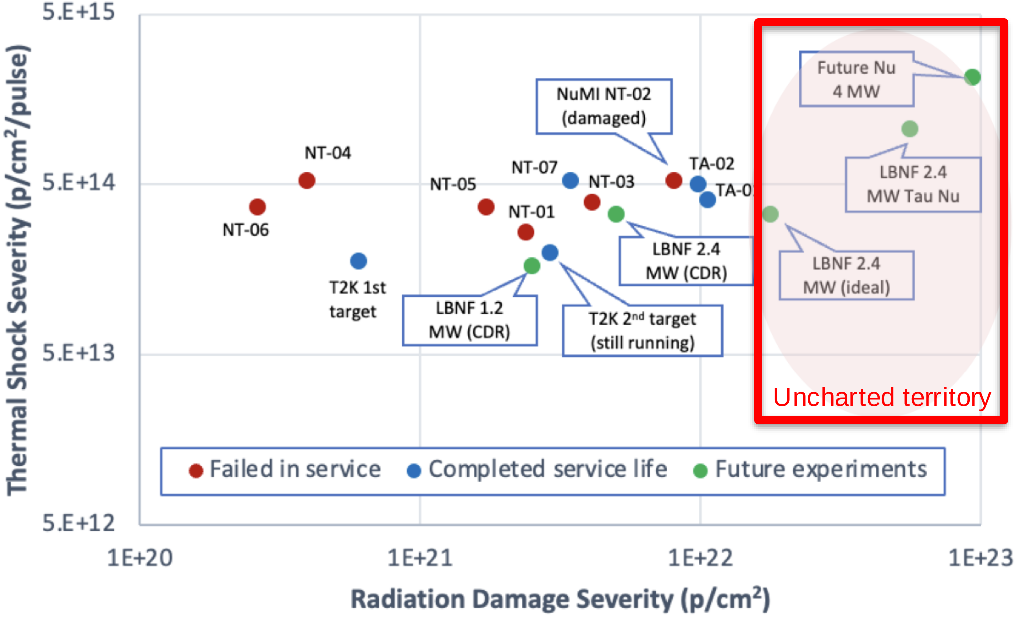

Fermilab

Radiation damage & thermal shock effects

Radiation damage:

- Hardening/embrittlement/creep
- Lattice expansion/void formation/bulk swelling
- Fracture toughness reduction
- Thermal/electrical conductivity reduction
- Coefficient of thermal expansion
- Modulus of elasticity
- Accelerated corrosion

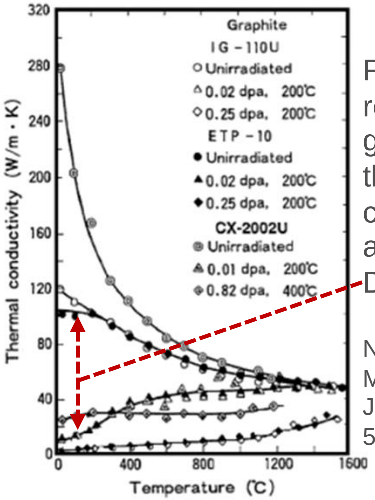

Factor of 10 reduction in graphite thermal conductivity after 0.02 DPA.

N. Maruyama, M. Harayama, JNM, 195, 44-50 (1992)

D.L. Porter and F. A. Garner, J. Nuclear Materials, **159**, p. 114 (1988)

Void swelling in 316 stainless steel, reactor dose of 1.5 x 10^{23} n/cm^2

Pulsed beam thermal shock

- E dep. → ΔT → dynamic stress wave
    - 1 MW target: 250 K in 10 µs (2.5 x 10^7 K/s)
    - Plastic deformation, cracking, fatigue failure

Material response dependent on:

- Specific heat (ΔT)
- Coefficient of thermal expansion (strain)
- Modulus of elasticity (stress)
- Flow stress behavior (plastic deformation)
- Strength (yield, fatigue, fracture toughness)

Sigraflex target tested at CERN's HiRadMat facility

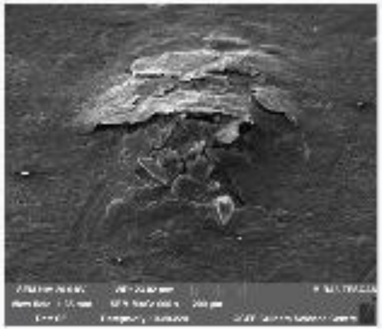

Test Iridium target irradiated at CERN's HiRadMat

What We Want to Avoid…

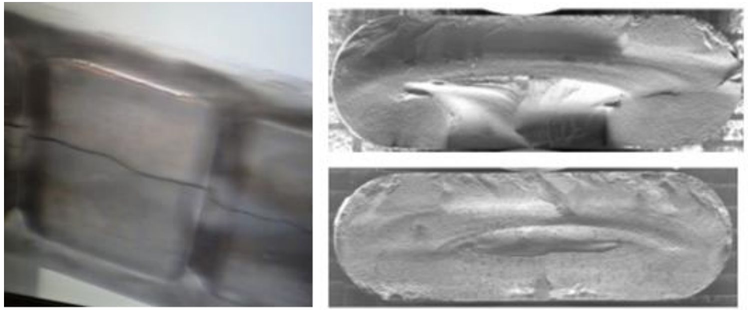

MINOS NT-02 target failure: radiation-induced swelling (FNAL)

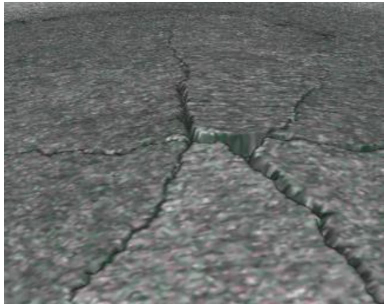

Be window embrittlement (FNAL)

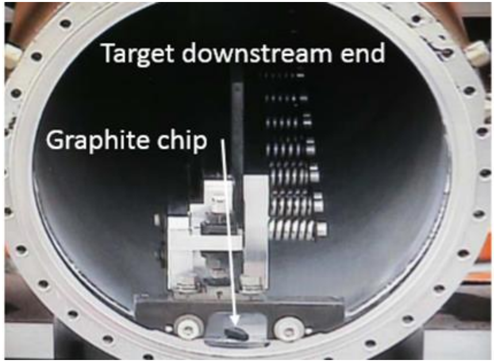

NOvA MET-01 target fin fracture (FNAL)

MINOS NT-01 target containment water leak (FNAL)

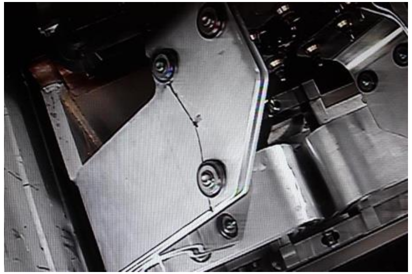

Horn stripline fatigue failure (FNAL)

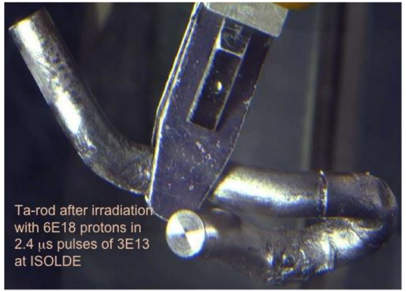

ISOLDE target (CERN)

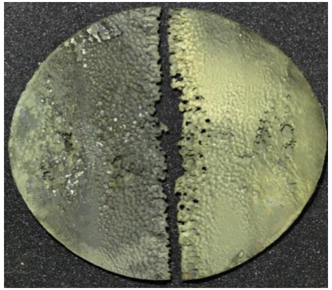

Target containment vessel cavitation (ORNL - SNS)

Neutrino Targets

MINOS (400 kW)

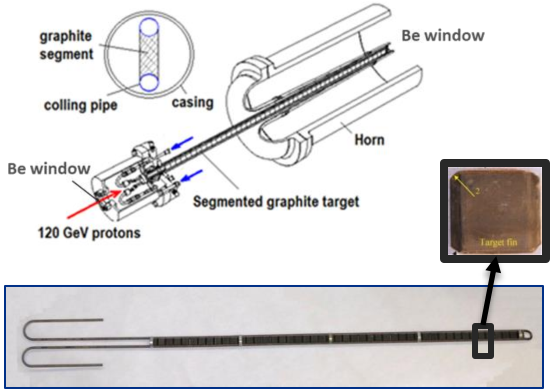

- Helium atmosphere
- Beryllium windows
- Water cooled graphite core

	MINOS
Graphite fins	47 x 20 mm x 6.6 mm
Beam energy [GeV]	120
p/pulse	3.37E+13
Power [kW]	340
σ [mm]	1.1
Peak Temp. [°C]	330
QS Temp [°C]	60
POT	6.55E+20
Peak dpa	0.63
Peak He [appm]	2270

NOvA (0.7 – 1 MW)

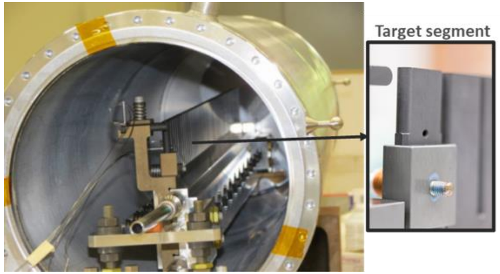

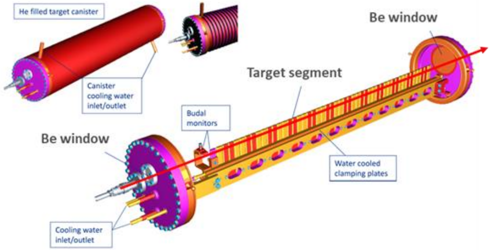

1 MW achieved (3 hr)!

- Helium atmosphere
- Beryllium windows
- Water cooled aluminum pressing plates
- Graphite core

	NOvA	AIP
Graphite fins	50 x 24 mm x 7.4 mm	50 x 24 mm x 9 mm
Beam energy [GeV]	120	120
p/pulse	4.90E+13	6.50E+13
Power [kW]	700	1000
σ [mm]	1.3	1.5
Peak Temp. [°C]	670	1000
QS Temp [°C]	390	890
POT	1.10E+21	1.28E+21
Peak dpa	1.10	0.96
Peak He [appm]	5580	3600

LBNF-DUNE (1.2 – 2.4 MW)

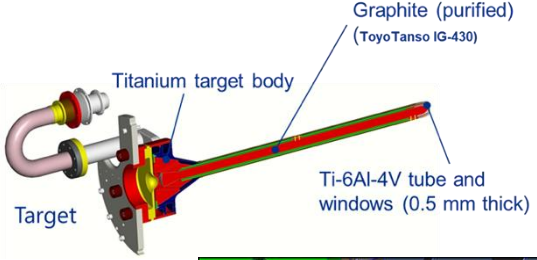

Concept 1.2 MW design

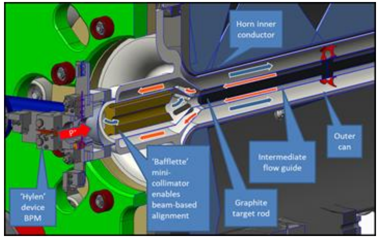

- Helium atmosphere
- Titanium target containment windows
- Helium gas cooled graphite core

	DUNE
Graphite fins	TBD
Beam energy [GeV]	60-120
p/pulse	7.50E+13
Power [kW]	1200-2400
σ [mm]	2.67
Peak Temp. [°C]	TBD
QS Temp [°C]	TBD
POT	2.54E+21
Peak dpa	0.73
Peak He [appm]	400

RaDIATE Collaboration

Neutrino High Power Targetry Materials (windows, production targets)

Created in 2012

Collaboration has grown to 20 institutions

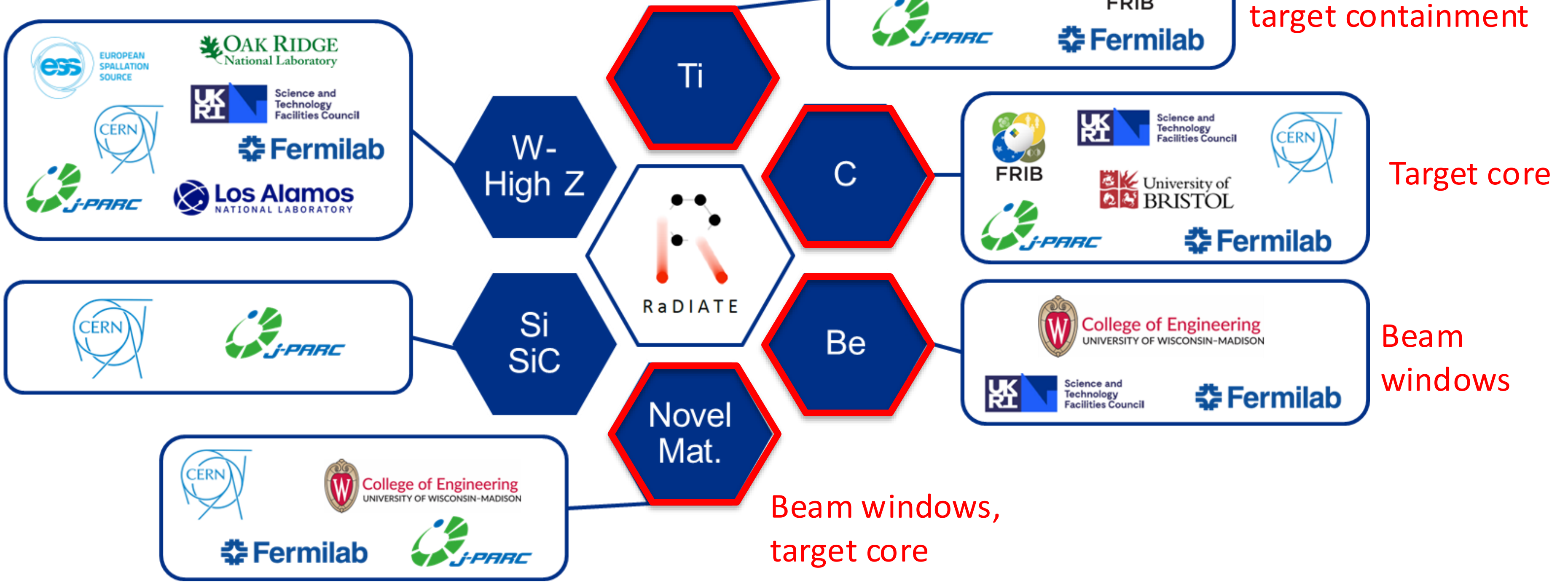

Research Approach - Prototypic irradiation to closely replicate material behavior in accelerator target facilities

- Analysis of in-beam accelerator components to directly test effects of high-energy, pulsed proton beams
- High-energy proton irradiation of material specimens at BNL-BLIP facility in partnership with the RaDIATE collaboration
  - Post-Irradiation Examination (PIE) at participating institution with hot-cell facilities (PNNL)
  - In-beam thermal shock experiment at CERN's HiRadMat facility including pre-irradiated (BLIP) and non-irradiated specimens
- Low energy ion irradiation to achieve high damage levels on short timescales and without activation

Fermilab

He implantation of Beryllium

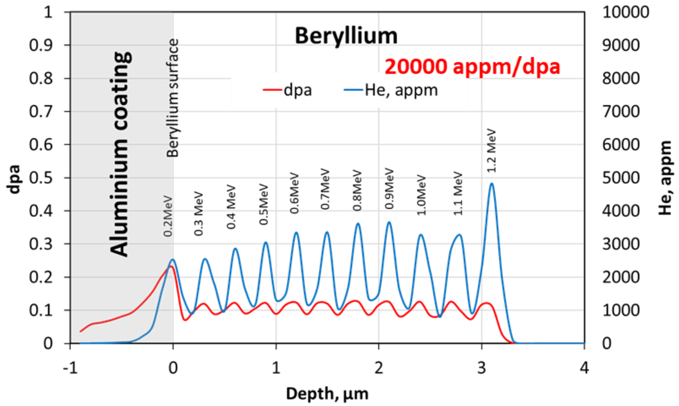

S. Kuksenko et al., J. Nuclear Materials, vol. 555, 15130, 2021

← 3 µm damage layer
T_{irrad}: 50 and 200 °C
0.1 DPA, 2000 appm He

Hardness of He-ion irradiated vs. non-irradiated Be samples →

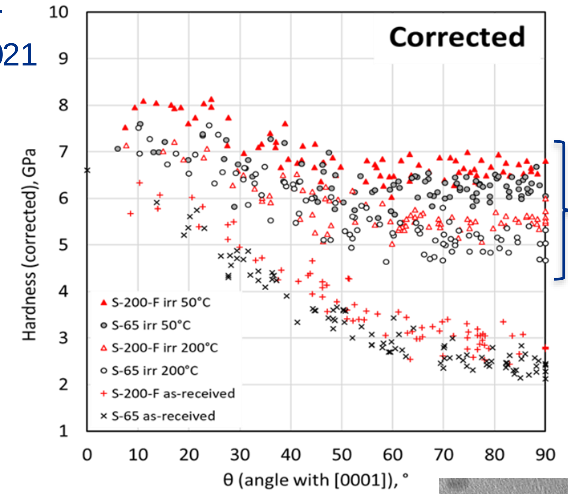

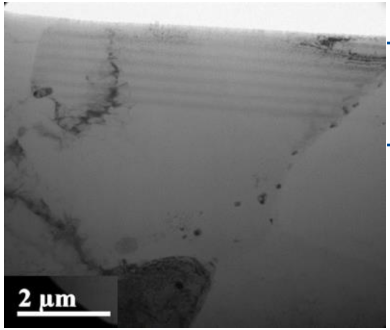

He implantation peaks

S. Kuksenko, RaDIATE Collaboration Meeting, 2019

- Helium produced at high rates in Be with high energy proton beams (~3000 appm/DPA)
- Low temperatures: He atoms do not diffuse
- High temperatures: He atoms become mobile
  → fill vacancy clusters & form damaging He bubbles
- He bubbles observed in NuMI Be window after **annealing** at 360 °C →
- However, higher temperatures are generally desired to anneal displacement damage (see hardness plot above)

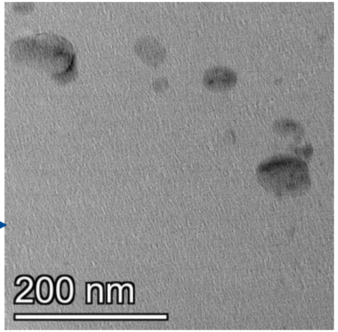

Fermilab

NuMI target (NT-02) autopsy and failure analysis

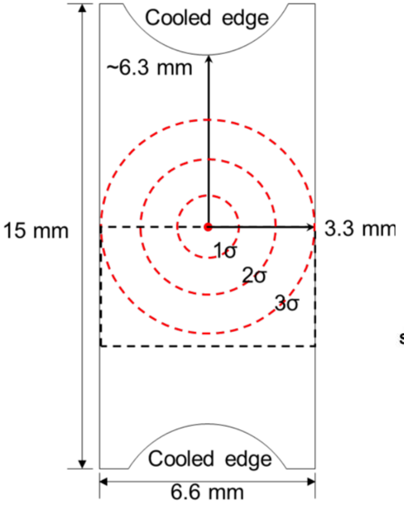

Beam Gaussian 1σ radius = 1.1 mm

- 340 kW, 120 GeV pulsed proton beam
- ΔT ~ 300° C over 10 μs
- Temperature gradient:
  ~370°C (beam center)
  ~60°C (cooled edge)
- Inert helium environment

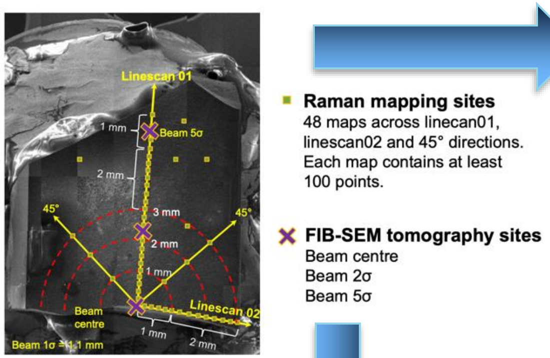

Stitched SEM image showing top-down view

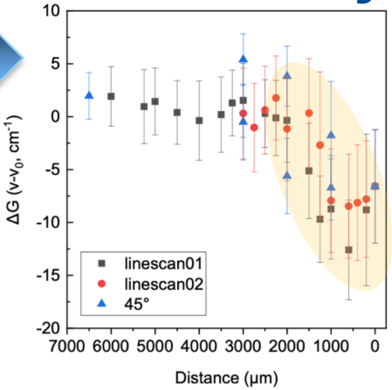

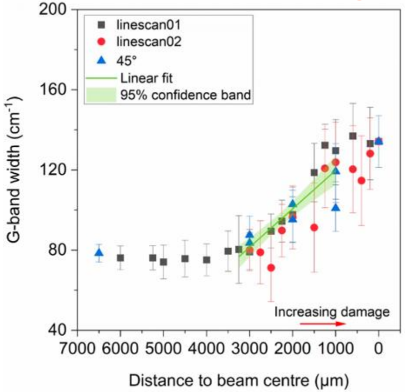

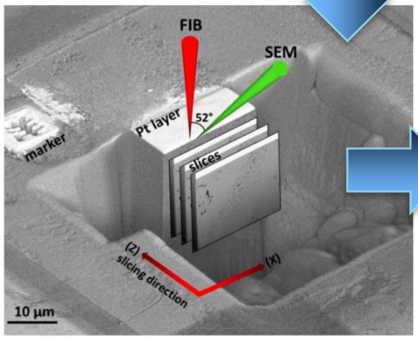

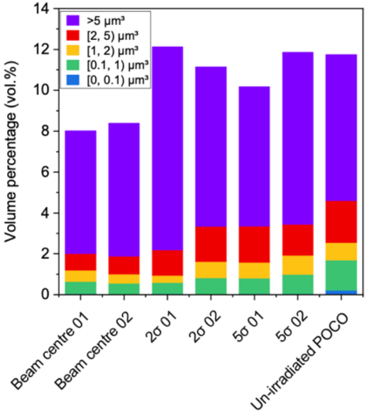

M. Jiang et al., Carbon 213 (2023) 118181

- D, G-band broaden at beam center
- Second order 2D-band gradually disappear
- *I(D)/I(G)* ratio stops increasing at high damage levels
- higher level of damage → significant broadening

- Total pore volume decreased from ~ 12 vol.% to ~ 8 vol.%
- Reduction of pores greater than 0.1 μm³ (bulk swelling)

High-Cycle Fatigue Testing of Irradiated Ti Alloys

Proton-irradiated fatigue life data crucial in evaluating component lifetime

- First high-cycle fatigue testing of irradiated Titanium at Fermilab
- Design of 3rd generation fatigue testing machine under development
- Complement prev. tensile tests on irradiated Ti

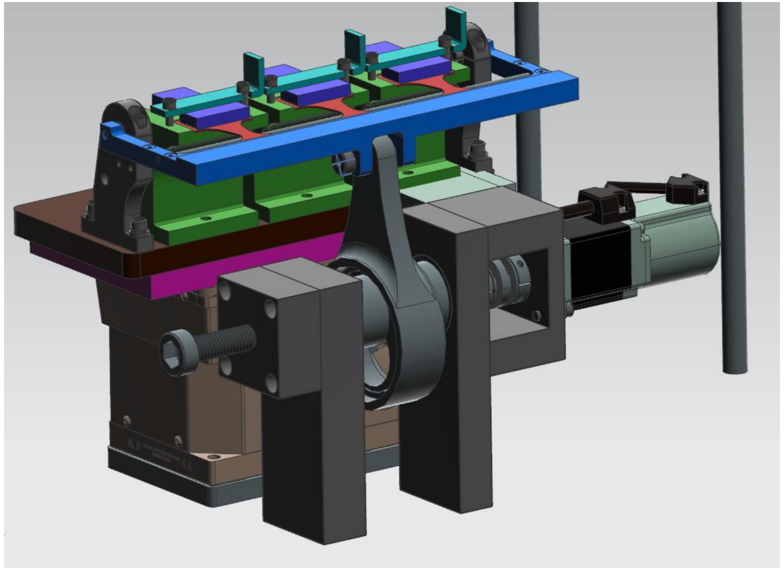

HRMT60 – RaDIATE experiment

~120 material specimens tested:

- Graphite, Ti alloys, Beryllium, Nanofiber mats, High-Entropy alloys, Sigraflex, TFGR tungsten, SiC/SiC composite
- Understand single-shot thermal shock response and limits
- Explore novel advanced materials
- Assess the performance of various grades of conventional materials
- Compare the behavior of non-irradiated to pre-irradiated materials
- Directly measure beam-induced dynamic effects to validate simulation

Beam Parameters	
Beam energy	440 GeV
Max. bunch intensity	1.2 x 10^{11}
No. of bunches	1 – 288
Max. pulse intensity	3.5 x 10^{13} ppp
Max. pulse length	7.2 μs
Gaussian beam size	1σ: 0.1 – 2 mm

Preliminary results:

- Visual inspection and high-resolution pictures of specimens
- Most of the samples didn't show track of beam damage except nanofiber specimen
- Predicted through heat transfer simulations in nanofiber media.

Nanofibers as production targets

Inherent resistance to radiation damage/thermal shock

- Radiation tolerance
  - Nanopolycrystalline grain structure
    - Absorb defects
  - In-situ ion irradiation & TEM: Argonne National Lab IVEM to 5 DPA
    - No observed damage
- Thermal shock
  - Discrete at microscale
  - Reduced temperature gradient (1D)
  - Heat dissipation in gas (high surface area & porosity)
  - Absorb/dampen stress waves
  - Survived test CERN's HiRadMat facility

(Bidhar et al., PRAB, 24, 2021)

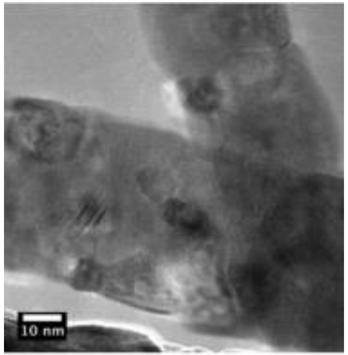

TEM before irrad.

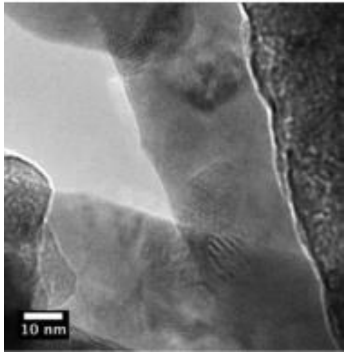

TEM after irrad.

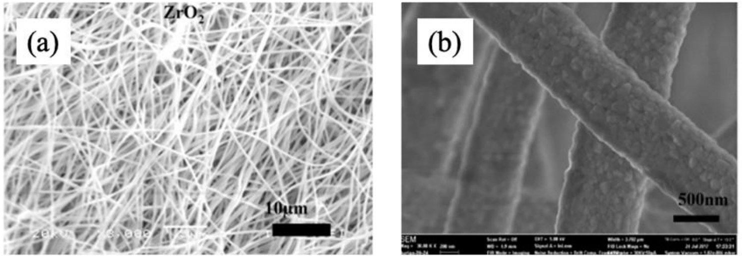

Zirconia nanofibers produced at Fermilab
(a) Bulk nanofiber mat
(b) Single nanofibers revealing polycrystalline grains

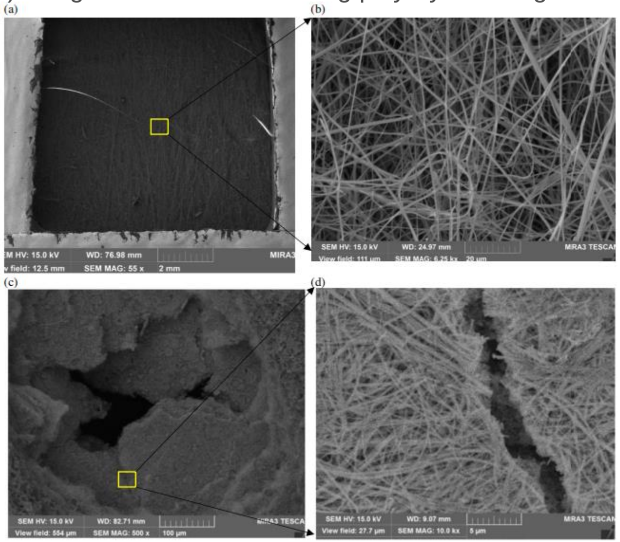

- Low packing density samples survived
- Holes, crack in higher density samples

Multiphysics Simulations of HRMT-43/60 Nanofiber Mats

ILLINOIS INSTITUTE OF TECHNOLOGY

Mesoscale ANSYS FLUENT simulation

Low packing density **High packing density**

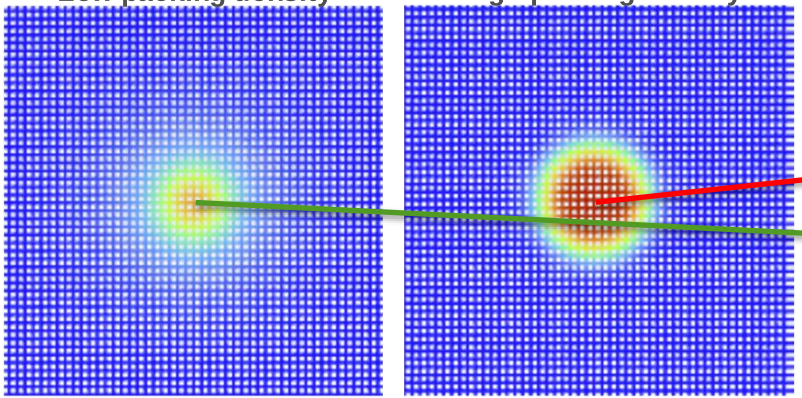

Pressure distribution at end of beam heating

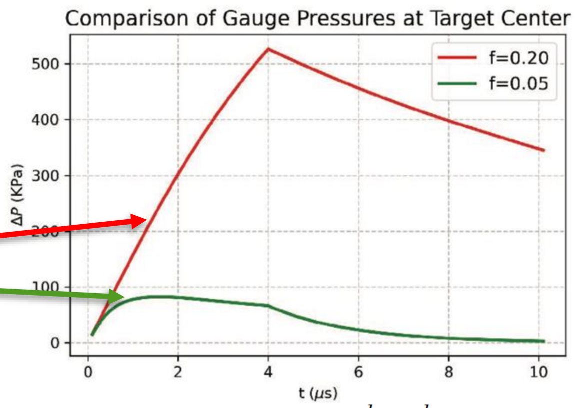

$$k_{\mathrm{eff}}(T) = k_0 + \frac{k_g - k_0}{1 + \frac{f}{1-f}\left[1 + \frac{5}{6}\frac{k_g - k_0}{k_g + k_0}\right]}$$

Will Asztalos (MS/PhD work, IIT)

Rapid heating

- Pressure wave for high packing dens.

Higher packing density

- Reduced airflow
- Greater pressure on fibers

Asztalos, W., et al. *arXiv preprint arXiv:2405.19496* (2024)

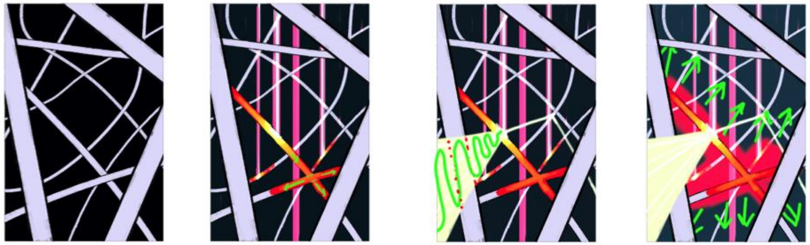

1. Start!

2. Beam hits: fibers instantly heat and conduction starts

3. Radiation is emitted from hot fibers

4. Helium around fibers heat, starts convection

Porous Media Models: three modes of heat transfer

- *Conduction:* introduce effective thermal conductivity $k(T)$ for nanofiber mat due to Bhattacharyya and Daryabeigi
- *Convection:* use Darcy's Law to simulate fluid flow, include energy equation in simulations
- *Radiation:* Mie Theory to solve scattering off infinite cylinder exactly, feed into model due to Lee

Fermilab

Pure W Nanofiber Fabrication

Initial SEM/EDS studies

- Presence of Oxygen (8 ~14 wt%)
- Also showed the presence of Carbon (black color)

Increased heat treatment temperature

- Reduced oxide formation
- Oxygen wt% dropped from 14% to 1.35%
- XRD analysis ongoing to evaluate crystal parameters, phase and structure

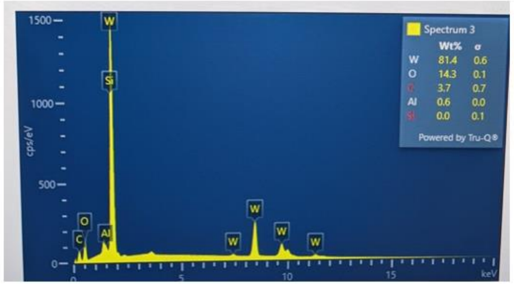

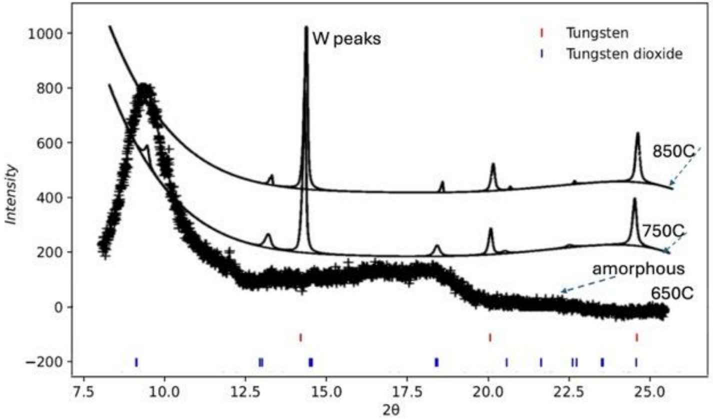

In-situ XRD of tungsten nanofibers during heat treatment (IMSERC facility – Northwestern University)

High *T* furnace with N2 gas flow

Element	Line Type	Apparent Concentration	k Ratio	Wt%	Wt% Sigma	Standard Label
C	K series	0.02	0.00022	16.43	5.99	C Vit
N	K series	0	0	0.33	4.18	BN
O	K series	0	0.00001	1.35	2.38	SiO2
Al	K series	0	0.00001	0.35	0.52	Al2O3
Si	K series	0	0.00003	0.52	1.13	SiO2
W	L series	0.44	0.00443	81.02	7.06	W
Total:				100		

EDS atomic composition results

HEA properties and compositions

Microstructure to combat radiation damage

- Sluggish atom diffusion
- Reduce defect segregation, increase recombination
- Phase stability

CALPHAD: CALculation of PHAse Diagrams

- Broad range: single-phase BCC
  - B2 precipitates: strengthening
- Low Z → reduce density
  - Decreased energy deposition and scattering

4 Gen. 1 compositions

- Varying number of alloying elements:
  - CrMnV → AlCoCrMnTiV

8 Gen. 2 compositions

- Study effects of different relative atomic concentrations

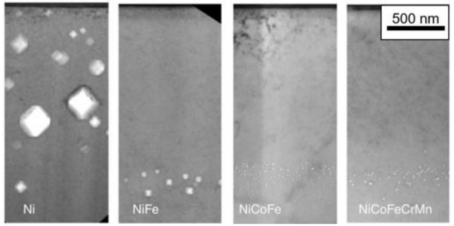

Void swelling lessened in more complex alloys (3-MeV Ni^{+}, 5 x $10^{16}/cm^2$, 773 K), Lu et al., Nature Comm., 2016

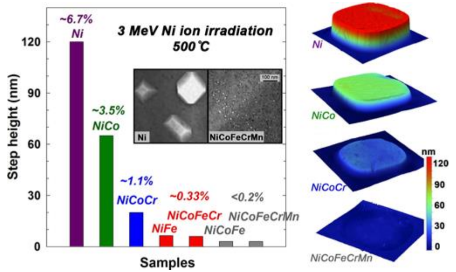

Swelling of increasingly complex alloys under ion irradiation, Jin et al., Scripta Materialia 119 (2016)

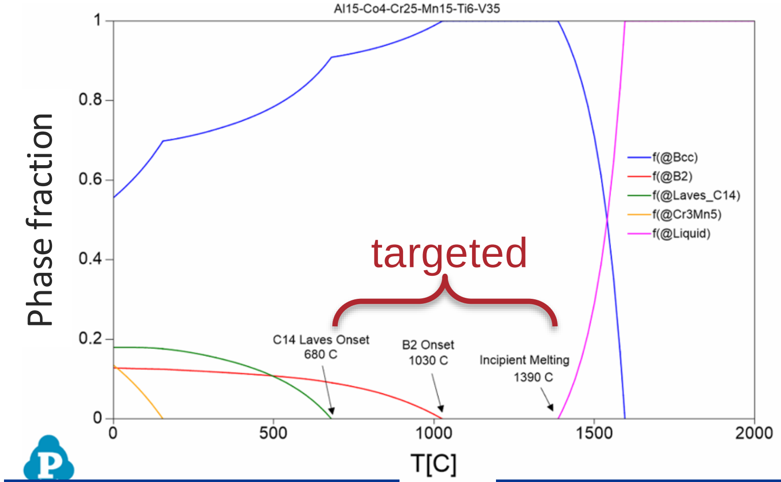

CrMnV Equimolar BCC single phase → **Ti** → **CrMnTiV** Impurity getter (<8%) → **Al** → **AlCrMnTiV** BCC phase stabilizer → **Co** → **AlCoCrMnTiV** Semi-coherent secondary phase

HEA homogeneity & impurity distribution

AlCoCrMnTiV

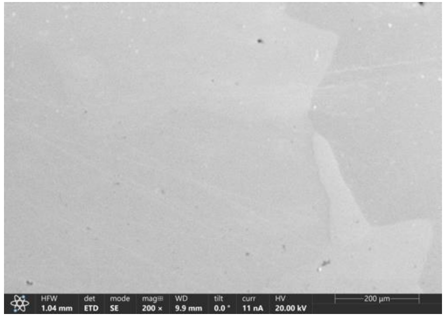

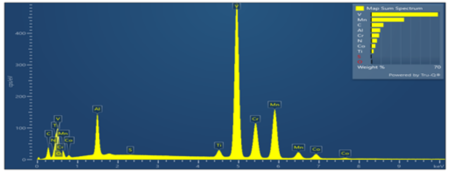

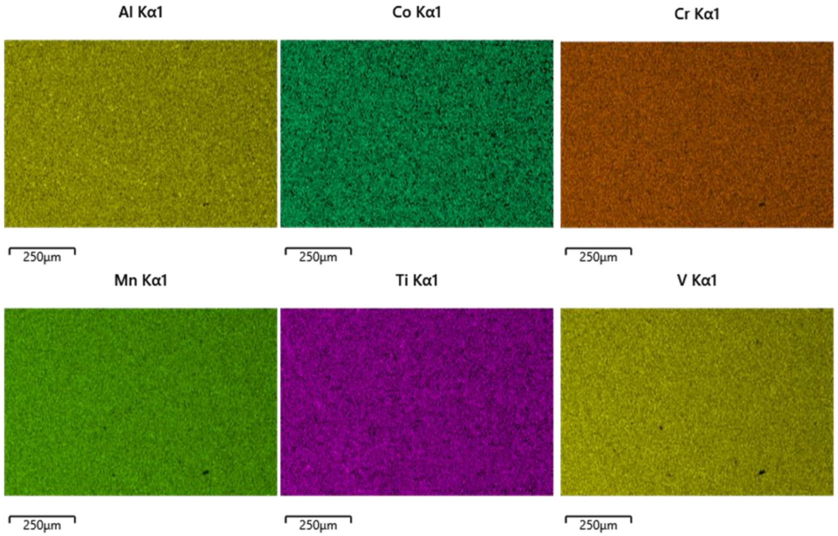

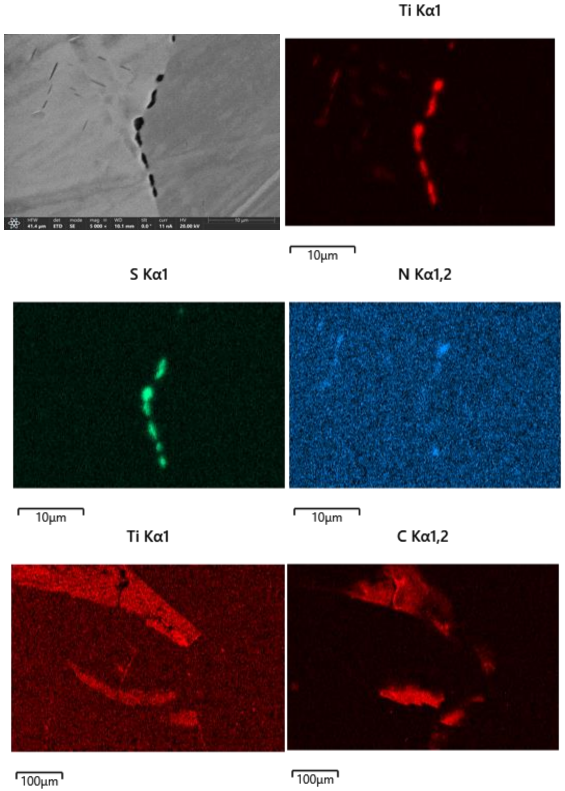

Energy Dispersive X-ray Spectroscopy (EDS)

- High degree of homogeneity observed in principal elements
- Ti working well as impurity getter
  - Captures C, N, O, S, predominantly at grain boundaries

Nanoindentation studies

N. Crnkovich, UW-Madison

College of Engineering
UNIVERSITY OF WISCONSIN–MADISON

Gen. 1
- Significant hardness increase with increased complexity (right)
  - Mitigated by heat treatment
- Signs of ductility
  - Stiffer than Ti-64 ($E = 110$ GPa)
  - Less stiff than Beryllium ($E = 303$ GPa)

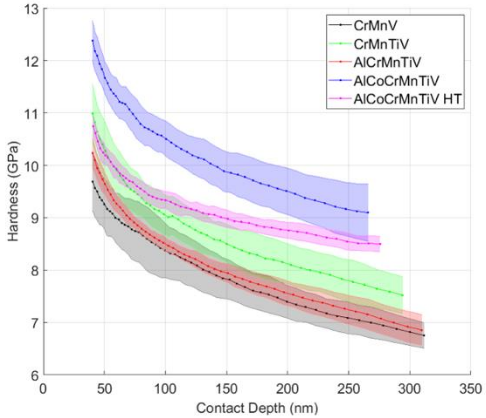

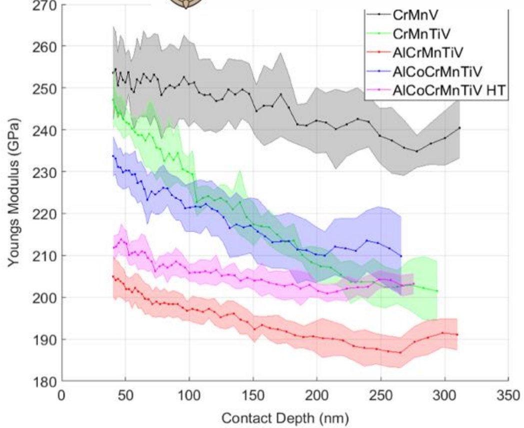

2nd Gen. micromechanical properties

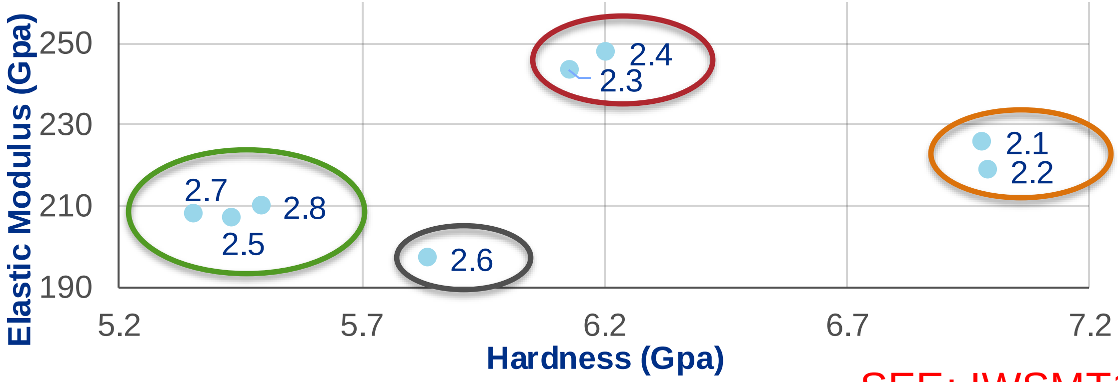

High Al/V, median Ti, no Cr

Low Al, median Ti

Median Al, low Ti/V

Low Al/Cr, high V

Gen. 2
- Lower hardness compared to Gen. 1
  - Increased ductility for high V content alloys
- Low dose 36 MeV Ar ion irrad. to 0.45 DPA
  - Irradiation induced softening observed

SEE: IWSMT16 presentation in October

Fermilab

Acknowledgements

- Fermilab HPT group: K. Ammigan, G. Arora, S. Bidhar, F. Pellemoine
- UW-Madison group: A. Couet, N. Crnkovich, M. Moorehead, I. Szufarska
- Illinois Institute of Technology: W. Asztalos, Y. Torun
- Work being done in the framework of the RaDIATE Collaboration (https://radiate.fnal.gov)
    - 80+ participants from 20 institutions worldwide
- Funded by DOE Early Career Award (Kavin Ammigan)

The work was supported by **Fermi National Accelerator Laboratory**, managed and operated by Fermi Research Alliance, LLC under Contract No. DE-AC02-07CH11359 with the U.S. DOE. This material is based upon work supported by the U.S. Department of Energy, Office of Science, Office of High Energy Physics under an **Early Career Research Program** award to KA. This project has received funding from the **European Union's Horizon Europe Research and Innovation programme**, under Grant Agreement No 101057511 (EURO-LABS)

Bonus slides

The NuMI Beam

Target station able to operate with 1-MW proton beam since FY21

- Future LBNF operation at 2.4+ MW

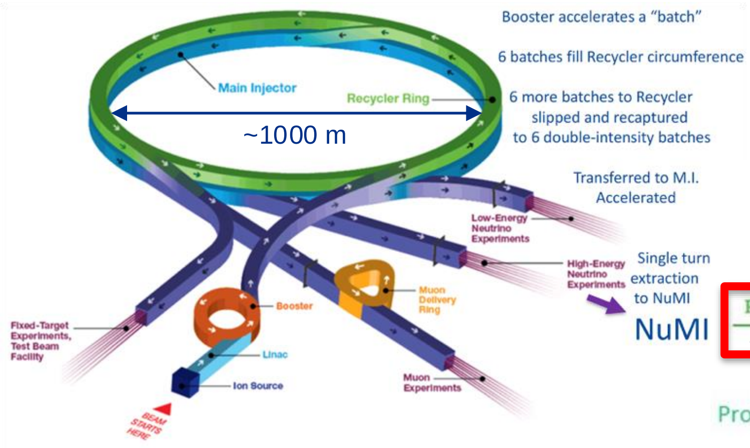

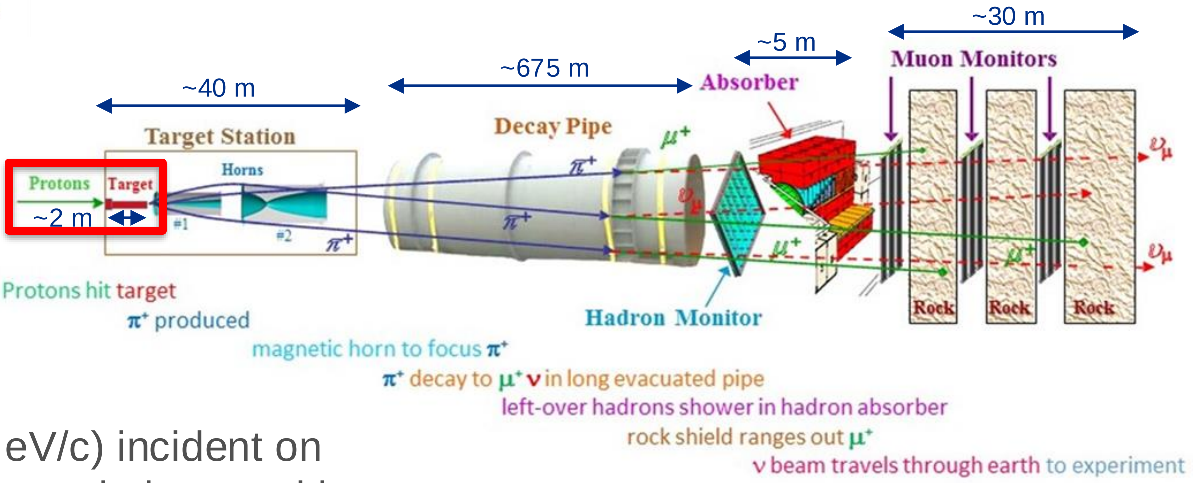

- Main injector proton beam (120 GeV/c) incident on 1.2 m graphite target to create charged pions and kaons.
- Pions focused in horns decay into muons/muon neutrinos in decay pipe to produce neutrinos.
- Beam detectors downstream of the decay pipe monitor the neutrinos produced and residual charged particles for the experiments.

Radiation damage process

Beam-induced damage

- Incident proton displaces target atoms
  - Causes damage cascade
  - Accumulated damage measured as Displacements Per Atom (DPA)

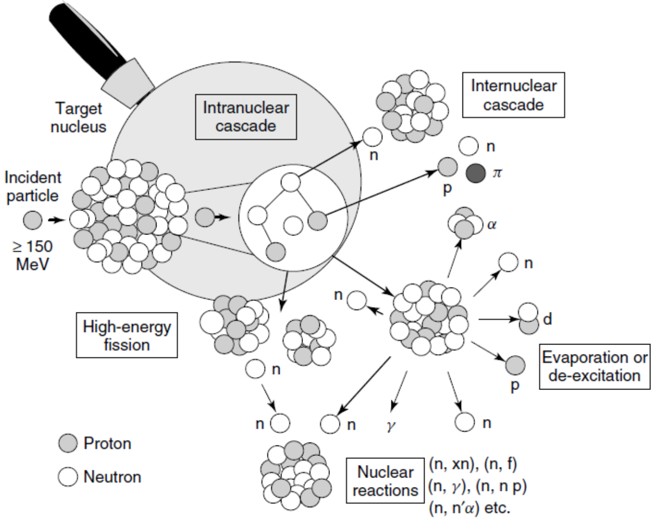

From D. Filges, F. Goldenbaum, in:, Handb. Spallation Res., Wiley-VCH Verlag GmbH & Co. KGaA, 2010, pp. 1–61.

Microstructure effects

- Creation of point defects (interstitial/vacancy)
- Transmutation products (H and He production)

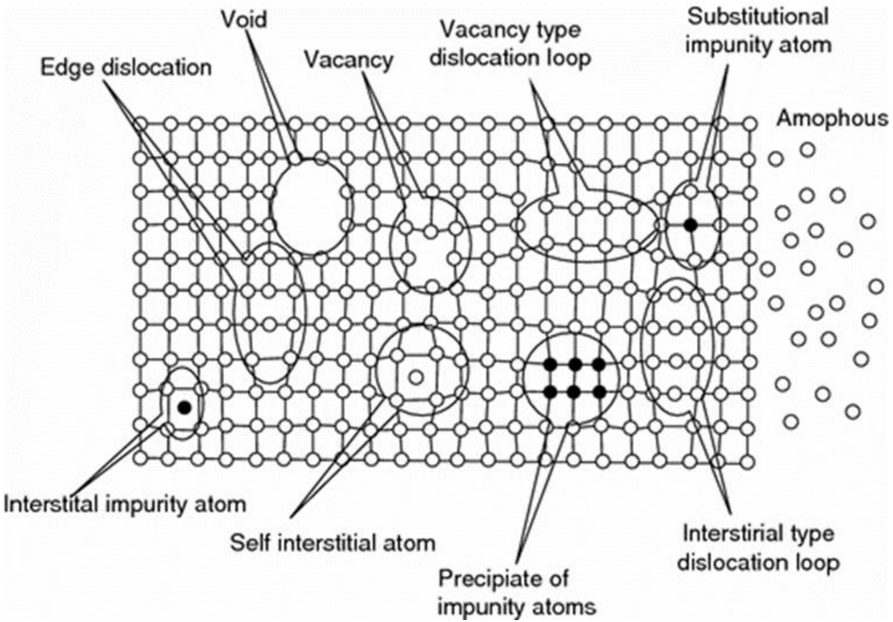

From V. Verma, K. Katovsky, Radiation Damage and Development of a MC Software Tool, in: Spent Nuclear Fuel and Accelerator-Driven Subcritical Systems, Springer, 2019.

Radiation damage bulk effects

Bulk effects:

- Hardening/embrittlement
- Creep
- Lattice expansion and bulk swelling
- Fracture toughness reduction
- Thermal/electrical conductivity reduction
- Coefficient of thermal expansion
- Modulus of elasticity
- Accelerated corrosion
- Void formation and embrittlement (due to transmutation)

N. Maruyama and M. Harayama, Journal of Nuclear Materials, 195, 44-50 (1992)

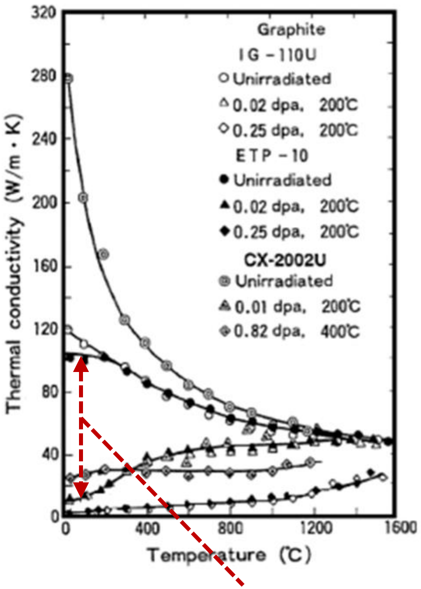

Factor of 10 reduction in thermal conductivity of graphite after 0.02 DPA

D.L. Porter and F. A. Garner, J. Nuclear Materials, **159**, p. 114 (1988)

Void swelling in 316 stainless steel tube exposed to reactor dose of 1.5 x 10^{23} n/cm^2

Thermal shock & stress waves

Pulsed beams: prompt E dep. → ΔT → dynamic stress wave

- Localized compressive stress
  - Fast expansion of material within cooler surrounding
  - 1 MW target: 250 K in 10 µs (2.5 x 10^7 K/s)
- Stress waves move at sonic velocities
- Can result in
  - Plastic deformation
  - Cracking
  - Fatigue failure

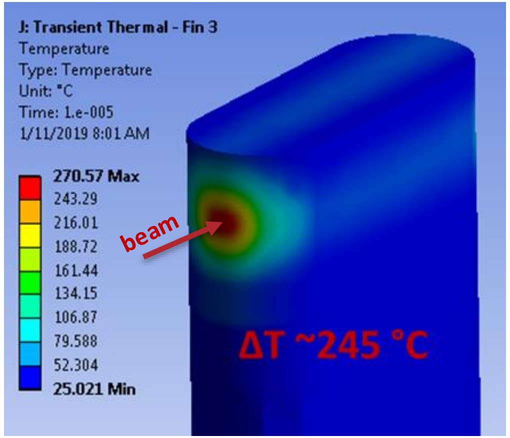

1 MW NuMI target simulation by K. Ammigan

Material response dependent on:

- Specific heat (ΔT)
- Coefficient of thermal expansion (strain)
- Modulus of elasticity (stress)
- Flow stress behavior (plastic deformation)
- Strength (yield, fatigue, fracture toughness)

$$\sigma = \sqrt{\rho E} \cdot \alpha \cdot L \cdot \frac{\Delta T}{\Delta t}$$

Initial stress wave amplitude

$$c = \sqrt{\frac{E}{\rho}}$$

Elastic wave speed

Sigraflex target tested at CERN's HiRadMat facility

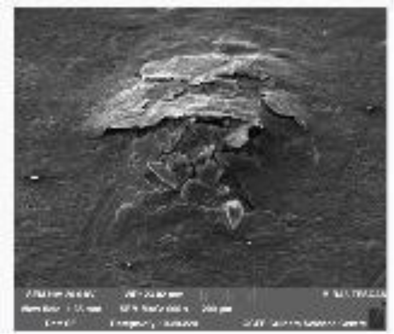

Test Iridium target irradiated at CERN's HiRadMat

Nanofibers as production targets

Inherent resistance to radiation damage and thermal shock

- Radiation tolerance
  - Nanopolycrystalline grains → absorb defects
- Thermal shock
  - Discrete at microscale
  - Reduced temperature gradient (1D)
  - Heat dissipation in gas (high surface area & porosity)
  - Absorb/dampen stress waves (discontinuity)

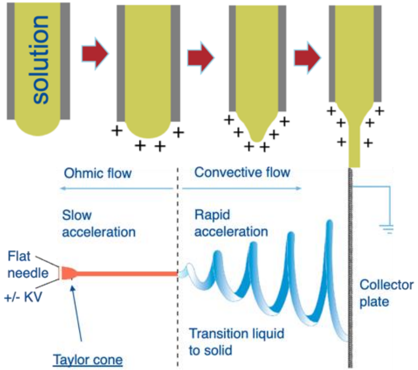

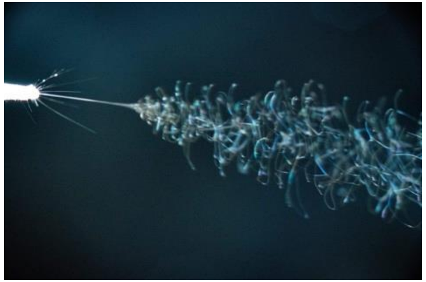

Photo: Reidar Hahn, FNAL

Electrohydrodynamic production of nanoscale fiber mats

- Electrostatic repulsion > surface tension
  - Droplet stretched
  - Jet elongated
- Zirconia nanofiber production in place
- Tungsten nanofibers under development

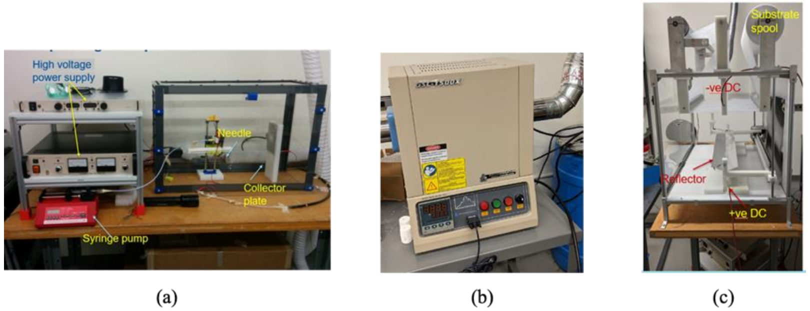

FNAL electrospinning setup: (a) Power supply and electrospinning set-up, (b) high-temperature furnace for nanofiber heat treatment, (c) roll-to-roll nanofiber fabrication technique

High entropy alloys (HEAs) for beam windows

- Alloy with 3+ principal elements
- Near equi-atomic compositions
- Primarily a solid-solution matrix with distorted crystal lattice (atomic size difference)
- Large composition space (adjustment of atomic ratios)

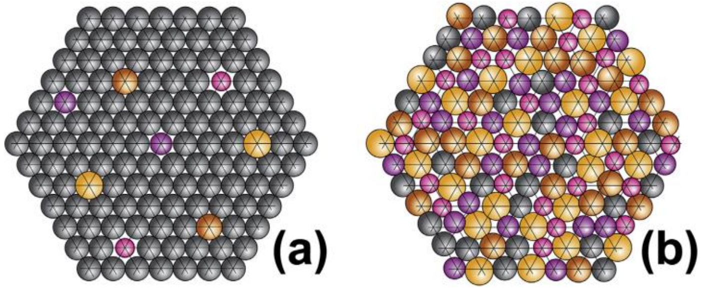

(a) Conventional Alloy, (b) High-entropy alloy
Miracle and Senkov, Acta Materialia 122 (2017) 448-511

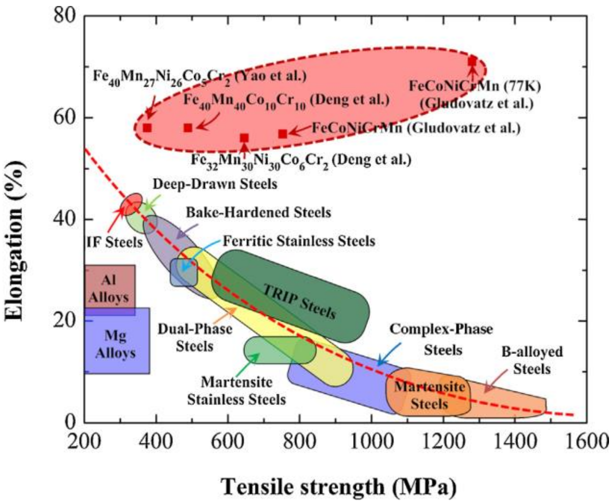

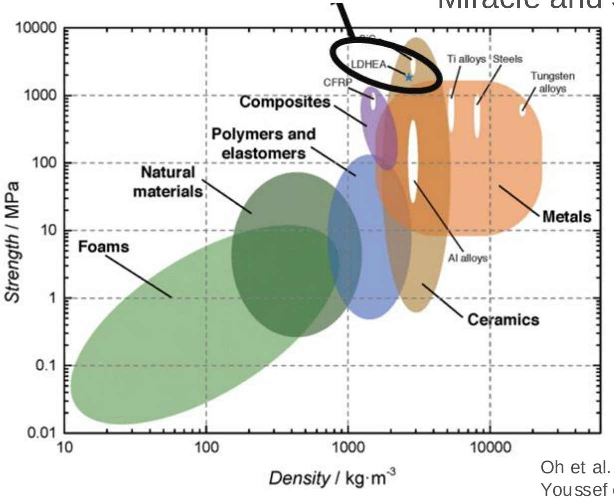

Many HEAs exhibit:

- Good ductility & high-temperature strength
- High strength to density ratio (specific strength)
- Fatigue, fracture, corrosion, oxidation resistance

Oh et al., Nat Comm. 10, 2090 (2019)
Youssef et al., Materials Research Letters, 95-99 (2015)

HEA radiation damage resistance

HEAs: microstructure to combat radiation damage

- Sluggish atom diffusion
  - distortion & size mismatch
  - Reduced segregation and defect clustering
  - Increased in-cascade recombination
- Phase stability
  - reduce grain coarsening and void swelling

Reduced defect segregation + increased recombination:

- Minimizes void formation & swelling (right, top)
- Reduces bulk swelling effects (right, bottom)
- Increasing # of elements → greater effects
  - vs. pure materials/traditional alloys
- Phonon scattering/migration energies

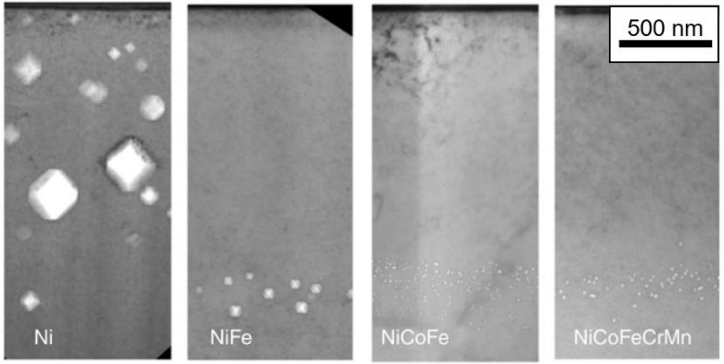

Void swelling shown to be less pronounced in more compositionally complex alloys upon heavy-ion irradiation (3-MeV Ni^{+} ions to 5 x 10^{16} cm-^{2} at 773 K), Lu et al., Nature Com., 2016

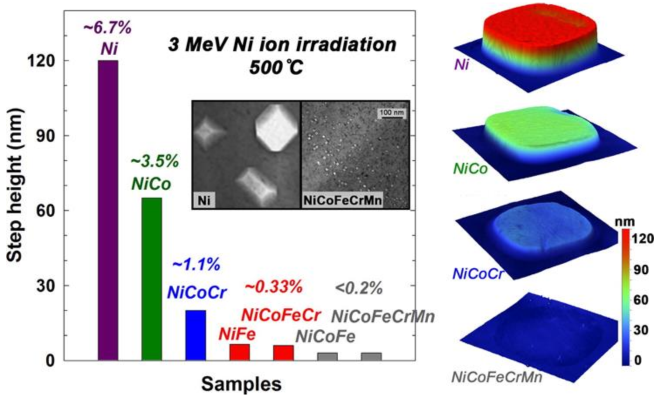

Swelling of increasingly complex alloys under ion irradiation, Jin et al., Scripta Materialia 119 (2016)

Fermilab

Simulations to determine HEA compositions

CALPHAD: CALculation of PHAse Diagrams

Select compositions with:

- Broad range: single-phase BCC
  - Increased ductility/machinability
  - B2 precipitates: strengthening
- Low Z → reduce density
  - Decreased energy deposition and scattering
  - Minimize beam loss in window

4 Gen. 1 compositions

- Varying number of alloying elements:
  - CrMnV → AlCoCrMnTiV

8 Gen. 2 compositions

- Study effects of different relative atomic concentrations

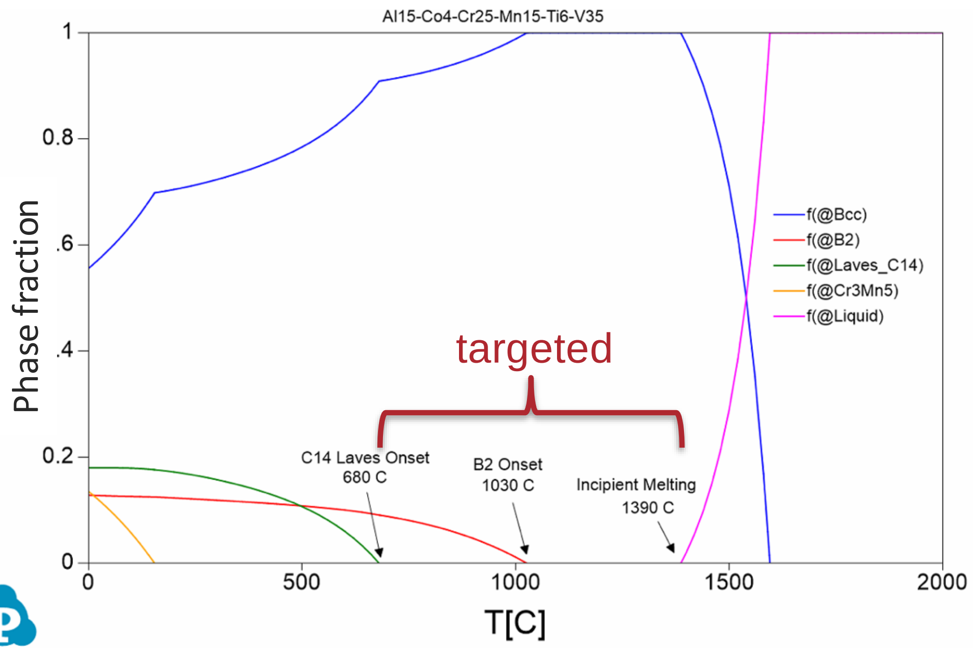

CrMnV
Equimolar BCC single phase

→ Ti →

CrMnTiV
Impurity getter (<8%)

→ Al →

AlCrMnTiV
BCC phase stabilizer

→ Co →

AlCoCrMnTiV
Semi-coherent secondary phase

Fermilab

HEA Synthesis

4 Gen. 1 HEA compositions

- Varying number of alloying elements:
  - CrMnV: Equimolar with single BCC phase
  - CrMnTiV: Ti as impurity getter
  - AlCrMnTiV: Al to stabilize BCC phase
  - AlCoCrMnTiV: Co for B2 precipitates

Sectioned arc-melted ingots (UW-Madison)

HEA samples sealed in quartz under vacuum before heat treatment (UW-Madison)

8 Gen. 2 compositions from Sophisticated Alloys to study effects of relative concentration

- 5 AlCoCrMnTiV compositions to study:
  - Varied Ti concentration as impurity getter
  - Varied Co concentration → secondary B2 phase
- Increased Al content without Cr
  - BCC phase stability
- Absence of Co
  - Al as B2 phase enhancer

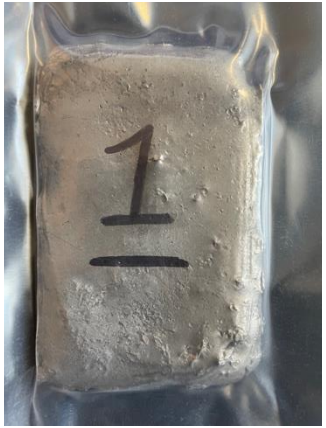

Gen. 2 plate from Sophisticated Alloys

Grain structure and orientation

Electron backscatter diffraction (EBSD)

- Mapping to determine grain sizes
- EBSD map shows grain sizes D ≈150 - 500 μm up to > 1mm
- Future study: nanoindentation orientation dependence

Helios 5 CX at FNAL

IPF Z Color 9

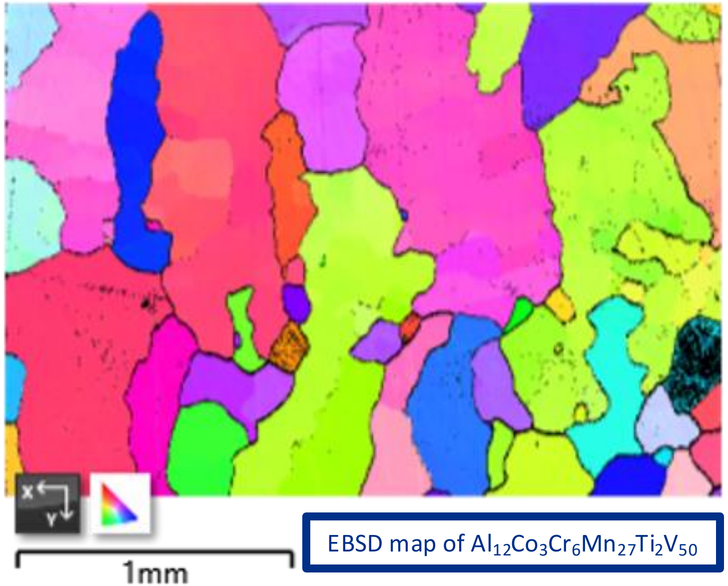

EBSD map of $Al_{12}Co_3Cr_6Mn_{27}Ti_2V_{50}$

$Al_{12}Co_3Cr_6Mn_{27}Ti_2V_{50}$ 20X optical

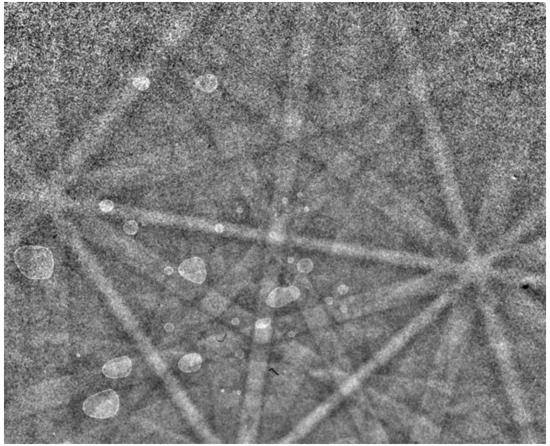

EBSD Kikuchi pattern

Elemental composition: Gen. 1

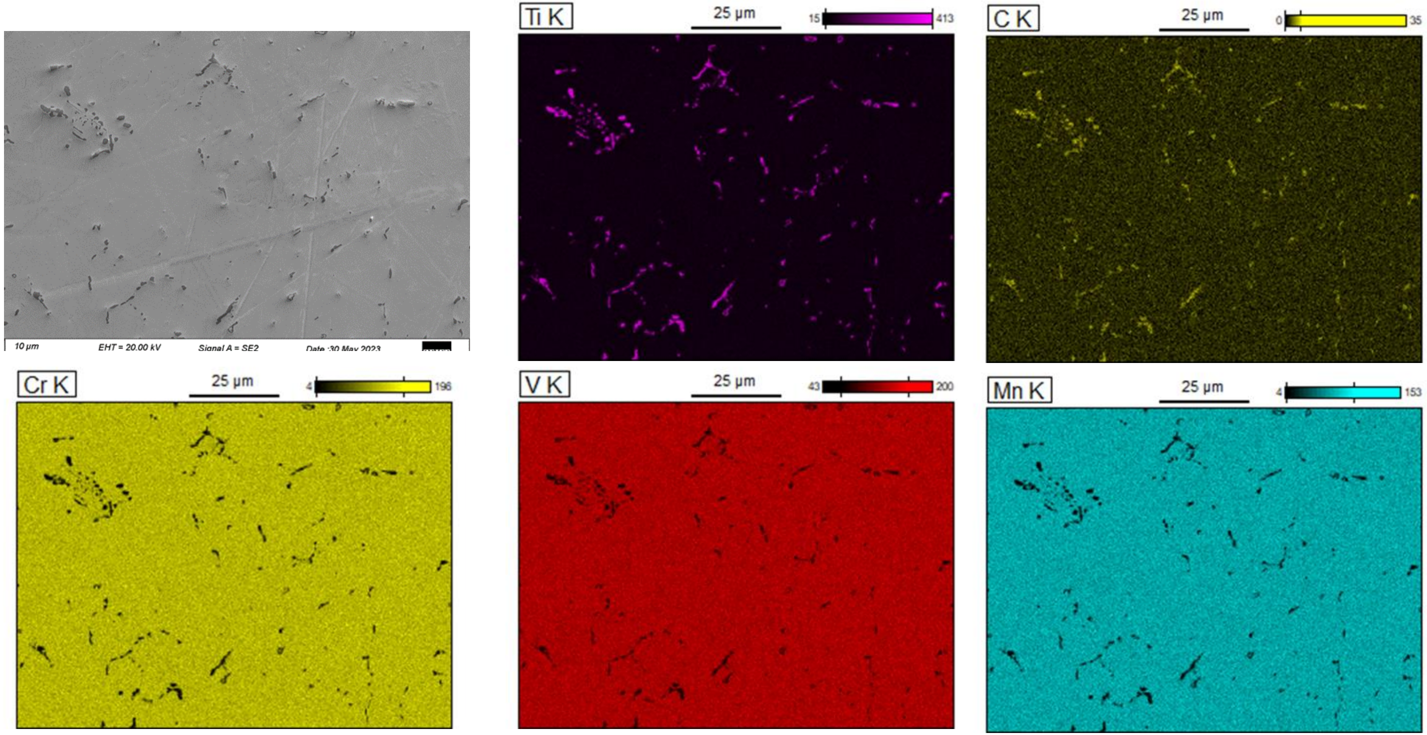

(N. Crnkovich, UW-Madison)

Energy dispersive spectroscopy (EDS) of CrMnTiV alloy

- Ti precipitates capture C impurities
- Cr, Mn, V show a very homogenous distribution

Mechanical properties following irradiation

Minimal hardening of CrMnV (< 5% at 100 DPA)

- Hardening of up to 30% in Ti-6Al-4V at 100 DPA
- Likely due to observed irradiation-induced voids and dislocations from TEM analysis

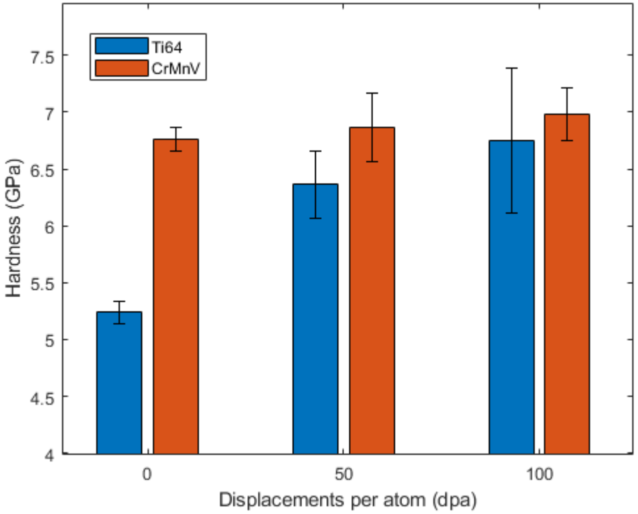

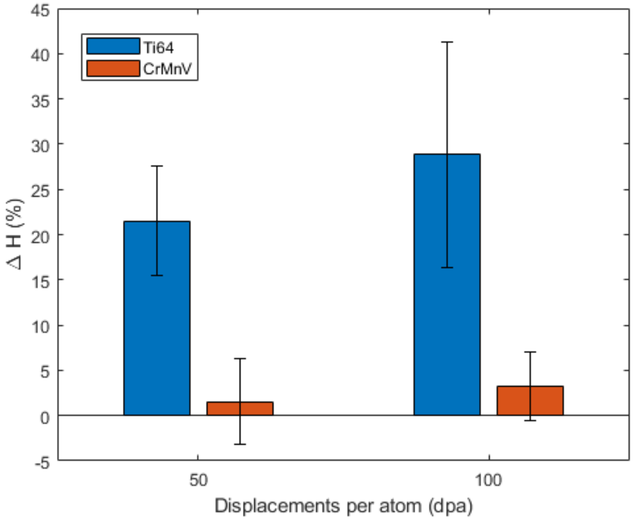

(N. Crnkovich, UW-Madison)

Crystal lattice structure and spacing

TEM completed on Gen. 1 alloys using FEI Tecnai TF-30 TEM (Nick Crnkovich, UW-Madison)

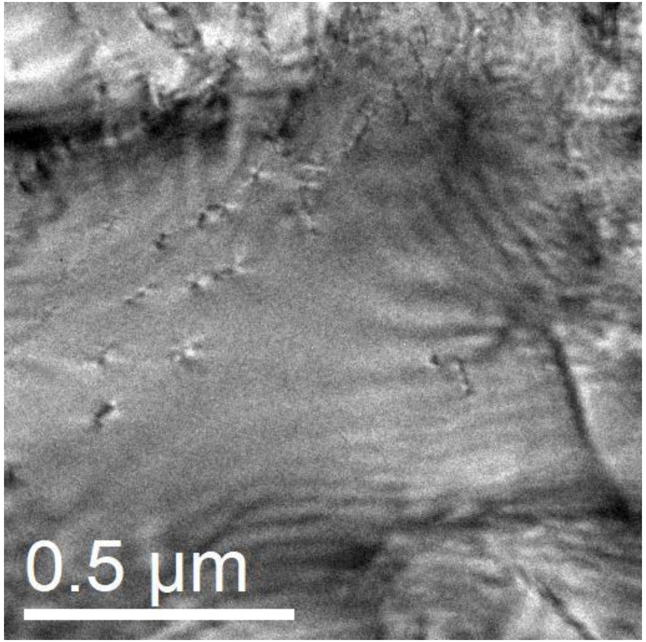

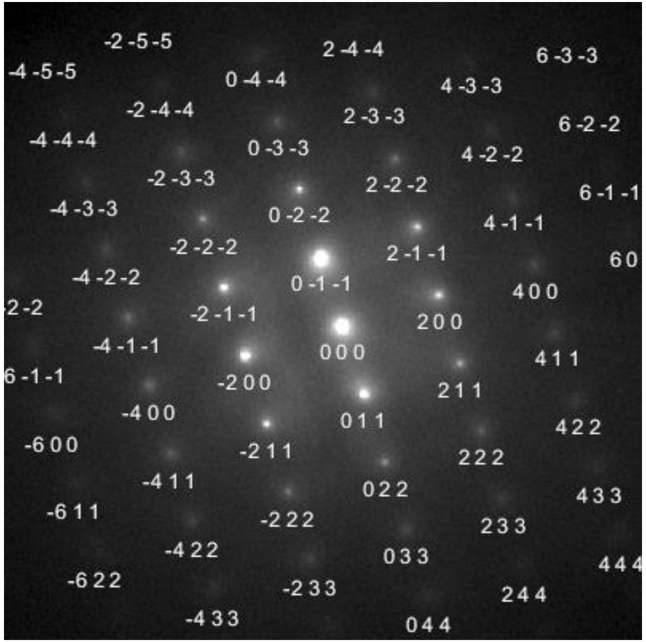

CrMnV: single phase BCC with d = 0.301 nm

Irradiation resistance testing

Post-irradiation TEM examination of Gen. 1 alloys
(Nick Crnkovich, UW-Madison)

- 50 and 100 DPA irradiated specimens
- Comparison to Ti-64 reference material

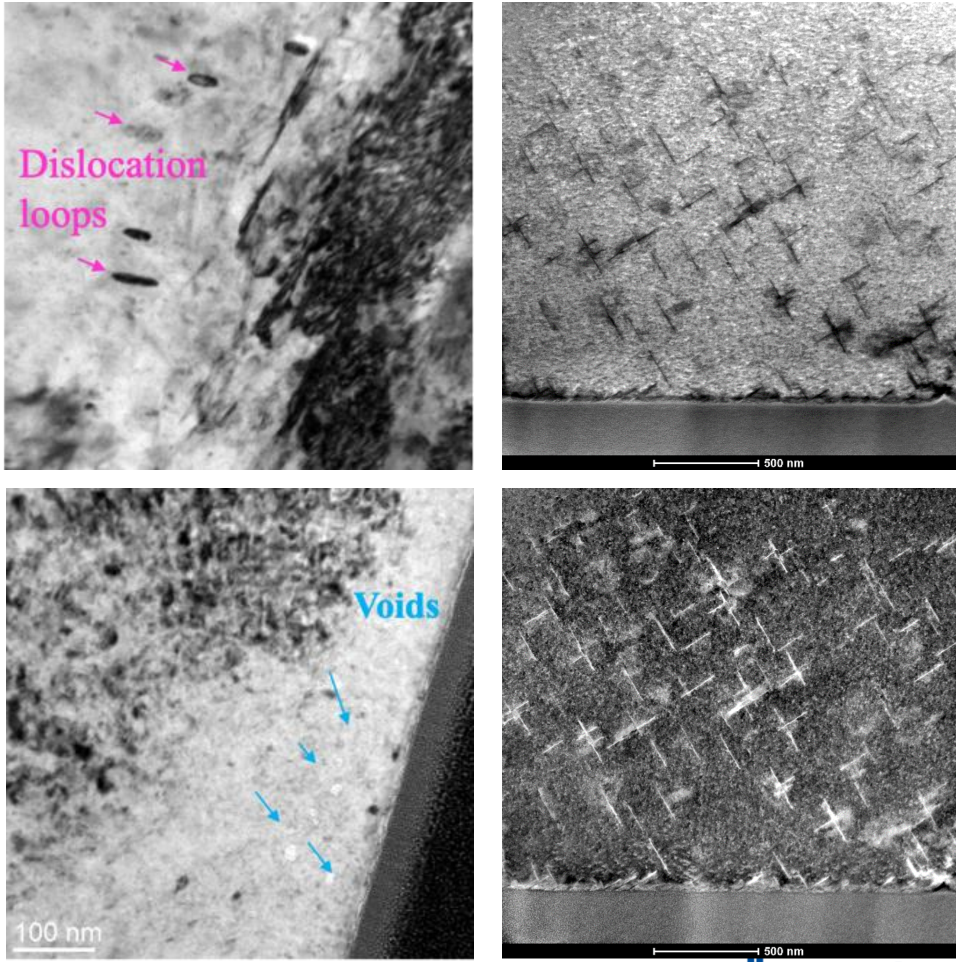

Ti-64 (left): many voids/dislocation loops observed at 50 DPA

→ not observed in CrMnV at 50 DPA (right)

- Needle morphology of CrMnV shows no chemical segregation

Crystal lattice structure and spacing

Transmission electron microscopy (TEM) at UW-Madison

Properties of interest

- Lattice spacing/expansion
  - Body centered cubic (BCC)
- B2 precipitates
  - Strengthening through dislocation pinning
- Transmission EDS
  - Composition of precipitates
- Irradiation induced defects

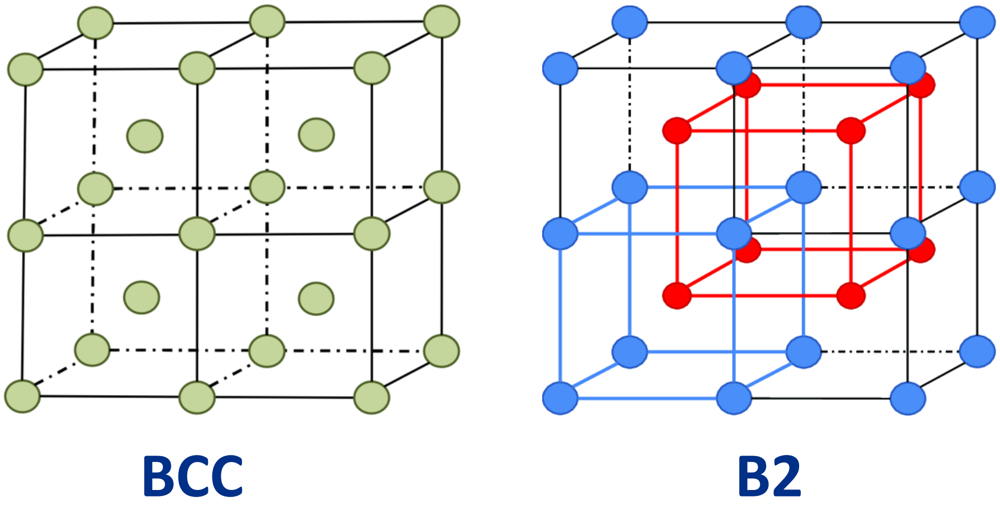

Lindahl, B. B., Burton, B. P., & Selleby, M. (2015). Ordering in ternary BCC alloys applied to the Al–Fe–Mn system. Calphad, 51, 211-219.

Precipitate identification in Gen. 2 HEAs

Gen. 2 TEM ongoing at UW-Madison

- Pristine samples initially
- 0.15, 0.30, 0.45, 5, and 10 DPA in future

$Al_{10}Co_4Cr_{25}Mn_{26}Ti_1V_{34}$ shown to right

- 10 – 30 nm precipitates observed
- Indexing to confirm phases awaits higher resolution images

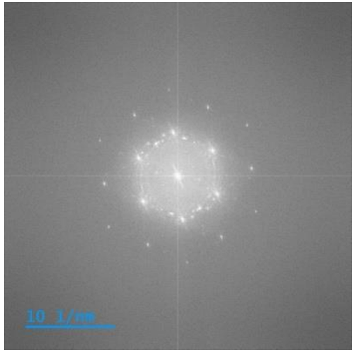

Diffractogram (FFT) of entire micrograph to right

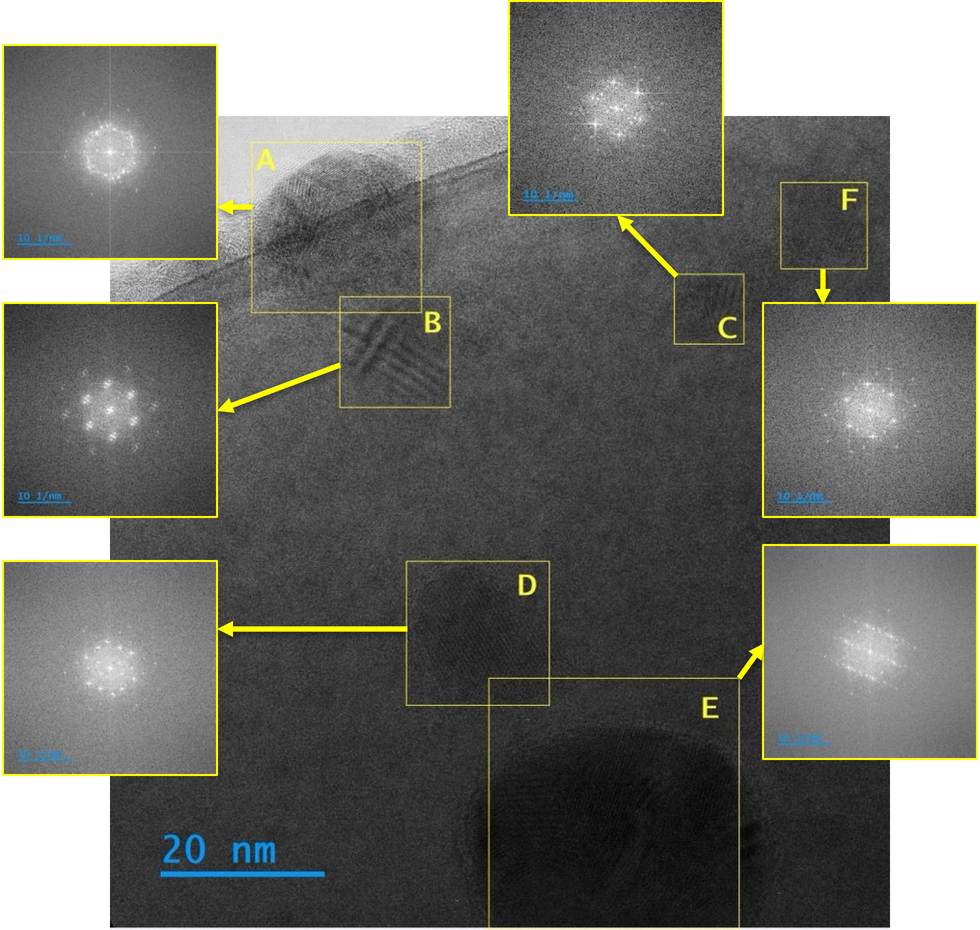

Fermilab

RaDIATE Collaboration

Radiation Damage In Accelerator Target Environments

RaDIATE collaboration created in 2012, with Fermilab as the leading institution. The collaboration has grown up to 20 institutions over the years.

Objective:

- Harness existing expertise in nuclear materials and accelerator targets
- Generate new and useful materials data for application within the accelerator and fission/fusion communities

Activities include:

- Analysis of materials taken from existing beamline as well as new irradiations of candidate target materials at low and high energy beam facilities
- In-beam thermal shock experiments

Contact:

- Frederique Pellemoine, fpellemo@fnal.gov
- Web: radiate.fnal.gov